Separatrix Reconnection and Meanders in the Standard Nontwist Map

A. Wurm, A. Apte, K. Fuchss, P.J. Morrison
Institute for Fusion Studies and Department of Physics
The University of Texas at Austin, USA

1. Introduction

In this paper we consider the *standard nontwist map* (SNM):[3]

$$\begin{aligned} x_{n+1} &= x_n + a\left(1 - y_{n+1}^2\right) , \\ y_{n+1} &= y_n - b\sin\left(2\pi x_n\right) , \end{aligned}$$

where $(x, y) \in \mathbb{T} \times \mathbb{R}$, $a \in (0, 1.5)$ and $b \in (-\infty, \infty)$. This is an *area-preserving* map that violates the *twist condition* along a curve in phase space. The SNM is *reversible*, i.e., it can be decomposed into involutions. The sets of fixed points of the involution maps are one-dimensional sets, called *symmetry lines* of the map. A major difference between the SNM and, e.g., the standard *twist* map is that there are two periodic orbits ("up" and "down"), if they exist, with the same winding number on each symmetry line.

Of particular interest is the so-called *shearless invariant curve*, which is invariant under the action of the reversing symmetry group of the SNM (see, e.g., Ref. 6), and exhibits strong resilience to perturbation. Previously, details of the break-up for several tori and their interpretation in terms of renormalization group operators have been studied.[1,2,4,5] Here our goal is a deeper understanding of the behaviour of the map in different regions of (a, b)-parameter space.

Nontwist maps are used to describe many physical systems, including the magnetic field lines in toroidal plasma devices such as reversed-shear tokamaks and stellarators (see Refs. 1 and 4 for bibliography). They are also of mathematical interest because, e.g., the KAM theorem and Aubry-Mather theory assume the twist condition.

Nontwist maps of the annulus exhibit interesting bifurcation phenomena: periodic orbit collision and separatrix reconnection. The latter is a global bifurcation that changes the phase space topology in the nontwist region. At the threshold of reconnection, the invariant manifolds of two or more distinct hyperbolic orbits with the same rotation number connect. Various aspects of this bifurcation have been studied over the years. For a much more exhaustive list of references see Ref. 13.

Here we highlight only a few recent developments: the occurence of meanders in the even-period orbit reconnection scenario[9] and some thoughts on shearless meanders in the odd-period reconnection. These ideas are explored in more detail in Refs. 12 and 13.

Key to the analytical and numerical exploration of the standard nontwist map is the map's invariance under symmetries. Of particular significance are the four *indicator points*,[9] fixed points of some of the symmetries of the SNM that always lie on the shearless curve. Shinohara and Aizawa devised a criterion to determine the approximate location in the (a, b)-parameter space of the breakup of shearless

invariant tori (see Ref. 8 for details). The boundary of the resulting break-up diagram [see Fig. 1(b)] displays a fractal-like structure. The analysis of Refs. 1,2,4, and 8 indicates that the highest peaks correspond to the break-up of shearless invariant tori with noble winding numbers. Subsequently, Shinohara and Aizawa proposed exact expressions, the *indicator curves*, for the bifurcation threshold of even-period hyperbolic orbits.[9] Indicator points were independently re-discovered by Petrisor[6] in the analysis of the reversing symmetry group of nontwist standard-like area-preserving maps.

2. Reconnection scenarios of even-period orbits

For orbits with even-period winding number, the up and down orbits on a symmetry line have the same stability type. The *standard* reconnection scenario, collision of hyperbolic points and formation of "dipoles" of elliptic points at the reconnection threshold, has been described in, e.g., Ref. 4.

In certain regions of (a, b)-parameter space the reconnection scenario changes. Phase space portraits [see, e.g., Fig. 1(a)] show the appearance of *meanders*, invariant tori that are not graphs over the x-axis, which are usually associated in the SNM with odd-period reconnection.[10,11]

Understanding the change in scenario requires the study of the indicator curves and the so-called *bifurcation curves* along the symmetry lines s_1 and s_3, first defined in the context of invariant torus break-up.[4] The *m/n-bifurcation curve* is the set of (a, b) values for which the m/n up and down periodic orbits are at the point of collision.

For most regions of (a, b) space the indicator curves and bifurcations curves (obtained using numerical methods described in Ref. 1) coincide. In regions close to bifurcation curves of odd-period orbits, bifurcation curves and indicator curves of even-period orbits diverge and even cross each other, as seen, e.g., in Fig. 1(b) for the 7/8-period orbit.

This change is due to a tangent-bifurcation along s_3 at the shearless point, which results in *new* pair of elliptic orbits of period 7/8 along s_3, together with a pair of hyperbolic points that move away from the symmetry axis. (For more details see Ref. 13.)

3. Global meanders, nested meanders, and meander transport

For the odd-period orbits the up and down periodic orbits on a symmetry line are of opposite stability type. As the orbits approach each other with increasing perturbation, the hyperbolic manifolds of the up and down orbits connect, leaving each hyperbolic orbit with a homoclinic and a heteroclinic manifold connection. In the region between the two chains, new periodic orbits and meanders appear, one of them shearless. Phase space plots of this scenario can be found, e.g., in Ref. 4. In some regions of parameter space manifold reconnection leads to global transport, and no meanders are created. (For details see Ref. 13.)

As a particular case consider the fixed points of the SNM, since their location is independent of (a, b). Thus even though the manifolds of the hyperbolic fixed points reconnect, the orbits never collide. The resulting meanders are dubbed "global meanders" because they can traverse large regions of phase space. Transport in phase

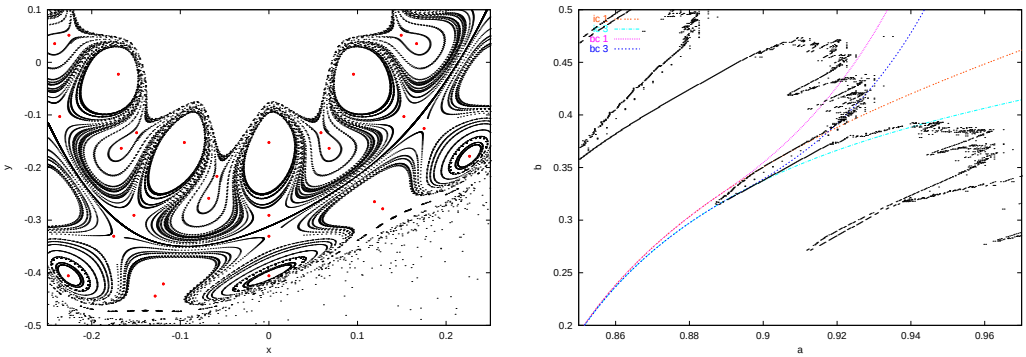

(a) Meanders during reconnection of 7/8 periodic orbits at $(a, b) = (0.926, 0.2297)$.

(b) Boundary for the breakup of shearless curves (dots), the indicator curves (ic1 and ic3) and bifurcation curves (bc1 and bc3) for 5/6 periodic orbits.

Figure 1:

space can occur *along* these tori even when they are not broken. The implications of such transport scenarios in applications such as the structure of magnetic field lines are being investigated (see Ref. 12 for more details and plots).

The winding number of meanders is less than that of the reconnecting orbits bordering the meandering region. Consequently the winding number profile attains a minimum, which corresponds to the shearless meander if the minimum winding number is irrational. If the perturbation is increased so that the minimum reaches a rational number, one can see the reconnection process occur locally inside the meandering region. A local maximum at the bottom of the minimum of the winding number plot indicates this "second order" reconnection, giving rise to "nested meanders". This is illustrated in Figs. 2(a)-2(b).

Thus we can imagine that the reconnection of periodic orbits inside this second order meandering region will lead to third order meanders.[10] If this process continues, then at certain "critical" parameter values b_c, the limiting curve will have structure at all scales even though it is not at the point of breakup. Even apart from the structure of such a higher order meander, it is still an open question whether the last curve to break is a shearless meander or a non-meandering curve.[6] An investigation of the breakup of meandering curves using Greene's residue criterion is under way.

Acknowledgments This research was in part supported by U.S. Department of Energy Contract No. DE-FG01-96ER-54346 and by an appointment of A. Wurm to the U.S. Department of Energy Fusion Energy Postdoctoral Research Program administered by the Oak Ridge Institute for Science and Education.

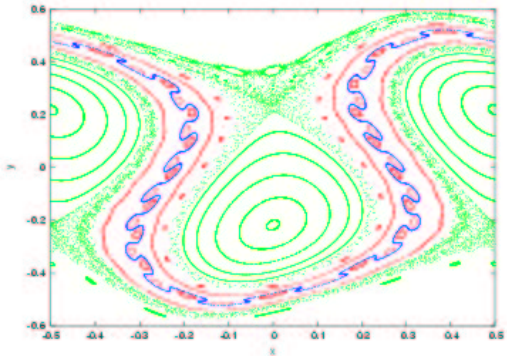

(a) Nested meanders around the 18/19 orbit inside the meandering region of 1/1 orbit.

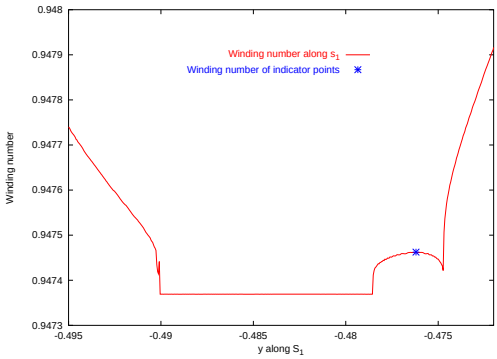

(b) The local maximum at the bottom of the local minimum, showing the presence of nested meanders. The "minimum" on the right should be at 18/19, the same value as the plateau.

Figure 2:

References

1. A. Apte, A. Wurm, and P. J. Morrison, Chaos **13**, 421 (2003).
2. A. Apte, A. Wurm, and P. J. Morrison, submitted to Physica D (also available at `http://www.ma.utexas.edu/mp_arc-bin/mpa?yn=03-466`).
3. D. Del-Castillo-Negrete and P. J. Morrison, Phys. Fluids A **5**, 948 (1993).
4. D. Del-Castillo-Negrete, J. M. Greene, and P. J. Morrison, Physica D **91**, 1 (1996).
5. D. Del-Castillo-Negrete, J. M. Greene, and P. J. Morrison, Physica D **100**, 311 (1997).
6. E. Petrisor, Int. J. of Bifur. and Chaos **11**, 497 (2001).
7. E. Petrisor, Chaos, Solit. and Fract. **14**, 117 (2002).
8. S. Shinohara and Y. Aizawa, Prog. Theor. Phys. **97**, 379 (1997).
9. S. Shinohara and Y. Aizawa, Prog. Theor. Phys. **100**, 219 (1998).
10. C. Simó, Regul. Chaotic Dyn. **3**, 180 (1998).
11. J. P. van der Weele, T. P. Valkering, H. W. Capel, and T. Post, Physica A **153**, 283 (1988).
12. A. Wurm, A. Apte and P. J. Morrison, Braz. J. Phys., to appear (2004) (also available at `http://www.ma.utexas.edu/mp_arc-bin/mpa?yn=04-45`).
13. A. Wurm, A. Apte, K. Fuchss and P.J. Morrison, in preparation (2004).